J|A|C|S
ARTICLES
Published on Web 07/11/2006

Synthesis, Characterization, and Self-Assembly of Pencil-Shaped CoO Nanorods

Kwangjin An,[†] Nohyun Lee,[†] Jongnam Park,[†] Sung Chul Kim,[†] Yosun Hwang,[‡] Je-Geun Park,[‡] Jae-Young Kim,[§] Jae-Hoon Park,[§] Myung Joon Han,[||] Jaejun Yu,[||] and Taeghwan Hyeon*[,†]

Contribution from the National Creative Research Initiative Center for Oxide Nanocrystalline Materials and School of Chemical and Biological Engineering, Seoul National University, Seoul 151-744, Korea, Department of Physics and Institute of Basic Science, Sungkyunkwan University, Suwon 440-746, Korea, Department of Physics and Pohang Light Source, Pohang University of Science and Technology, Pohang 790-784, Korea, and School of Physics and CSCMR, Seoul National University, Seoul 151-747, Korea

Received February 6, 2006; E-mail: thyeon@snu.ac.kr

Abstract: We synthesized uniformly sized, pencil-shaped CoO nanorods by the thermal decomposition of a cobalt−oleate complex, which was prepared from the reaction of cobalt chloride and sodium oleate. The diameters and lengths of the CoO nanorods were easily controlled by varying the experimental conditions, such as the heating rate and the amount of Co−oleate complex. The X-ray diffraction pattern revealed that the CoO nanorods have an extraordinary wurtzite ZnO crystal structure. These uniformly sized nanorods self-assembled to form both horizontal parallel arrangements and perpendicular hexagonal honeycomb superlattice structures. Reduction of the nanorods by heating under a hydrogen atmosphere generated either hcp Co or Co_2C nanorods. Characterization of the CoO nanorods using X-ray absorption spectroscopy, X-ray magnetic circular dichroism spectroscopy, and magnetic measurements showed that they contain a small fraction of ferromagnetic Co impurities.

Introduction

Magnetic nanocrystals have attracted a tremendous amount of attention from researchers in various disciplines, not only for their fundamental size-dependent magnetism but also for their many technological applications, including magnetic storage media, ferrofluids, contrast agents for magnetic resonance imaging, and magnetic carriers for drug targeting.[1] For many of these applications and fundamental studies, magnetic nanocrystals with a uniform and controllable particle size and shape are desirable.[1h] Uniformly sized cobalt nanocrystals with various crystal structures, particle shapes, and sizes have been synthesized using several chemical synthetic procedures, including the reduction of metal salts and the thermal decomposition of organometallic compounds.[2] Murray, Sun, and their coworkers at IBM synthesized spherical cobalt nanocrystals with various crystal structures, including ϵ-phase, face-centered cubic (fcc), and hexagonal close-packed (hcp).[2a] Recently, uniformly sized one-dimensional (1-D) nanostructures such as nanorods have received much attention because of their unique properties, which are derived from their dimensional anisotropy.[3] The Chaudret group reported the synthesis and self-assembly of uniformly sized cobalt nanorods from the decomposition of a

[†] National Creative Research Initiative Center for Oxide Nanocrystalline Materials and School of Chemical and Biological Engineering, Seoul National University.

[‡] Department of Physics and Institute of Basic Science, Sungkyunkwan University.

[§] Department of Physics and Pohang Light Source, Pohang University of Science and Technology.

[||] School of Physics and CSCMR, Seoul National University.

(1) (a) Schmid, G. *Nanoparticles: From Theory to Application*; Wiley-VCH: Weinheim, 2004. (b) Klabunde, K. J. *Nanoscale Materials in Chemistry*; Wiley-Interscience: New York, 2001. (c) Fendler, J. H. *Nanoparticles and Nanostructured Films*; Wiley-VCH: Weinheim, 1998. (d) Fertman, V. E. *Magnetic Fluids Guide Book: Properties and Applications*; Hemisphere Publishing Co.: New York, 1990. (e) Berkovsky, B. M.; Medvedev, V. F.; Krakov, M. S. *Magnetic Fluids: Engineering Applications*; Oxford University Press: Oxford, 1993. (f) Ziolo, R. F.; Giannelis, E. P.; Weinstein, B. A.; O'Horo, M. P.; Ganguly, B. N.; Mehrotra, V.; Russel, M. W.; Huffman, D. R. *Science* **1992**, *257*, 219. (g) Alivisatos, A. P. *Science* **1996**, *271*, 933. (h) Hyeon, T. *Chem. Commun.* **2003**, 927. (i) Zhang, J. Z.; Wang, Z.-L.; Liu, J.; Chen, S.; Liu, G.-Y. *Self-Assembled Nanostructures*; Kluwer Academic/Plenum Publishers: New York, 2003. (j) Pacholski, C.; Kornowski, A.; Weller, H. *Angew. Chem., Int. Ed.* **2002**, *41*, 1188.

(2) (a) Sun, S.; Murray, C. B. *J. Appl. Phys.* **1999**, *85*, 4325. (b) Dumestre, F.; Chaudret, B.; Amiens, C.; Fromen, M.-C.; Casanove, M.-J.; Renaud, P.; Zurcher, P. *Angew. Chem., Int. Ed.* **2002**, *41*, 4286. (c) Dumestre, F.; Chaudret, B.; Amiens, C.; Respaud, M.; Fejes, P.; Renaud, P.; Zurcher, P. *Angew. Chem., Int. Ed.* **2003**, *42*, 5213. (d) Osuna, J.; Caro, D.; Amiens, C.; Chaudret, B.; Snoeck, E.; Respaud, M.; Broto, J.-M.; Fert, A. *J. Phys. Chem.* **1996**, *100*, 14571. (e) Puntes, V. F.; Krishnan, K. M.; Alivisatos A. P. *Science* **2001**, *291*, 2115. (f) Puntes, V. F.; Gorostiza, P.; Aruguete, D. M.; Bastus, N. G.; Alivisatos, A. P. *Nat. Mater.* **2004**, *3*, 263. (g) Puntes, V. F.; Krishnan, K. M.; Alivisatos, A. P. *Appl. Phys. Lett.* **2001**, *78*, 2187. (h) Pileni, M. P. *J. Phys. Chem. B* **2001**, *105*, 3358. (i) Petit, C.; Taleb, A.; Pileni, M. P. *J. Phys. Chem. B* **1999**, *103*, 1805. (j) Petit, C.; Cren, T.; Roditchev, D.; Sacks, W.; Klein, J.; Pileni, M. P. *Adv. Mater.* **1999**, *11*, 1198. (k) Legrand, J.; Petit, C.; Pileni, M. P. *J. Phys. Chem. B* **2001**, *105*, 5643. (l) Shafi, K. V. P. M.; Gedanken, A.; Prozorov, R. *Adv. Mater.* **1998**, *10*, 590. (m) Russier, V.; Petit, C.; Pileni, M. P. *Phys. Rev. B* **2000,** *62*, 3910. (n) Lin, X. M.; Sorensen, C. M.; Klabunde, K. J.; Hadjipanayis, G. C. *Langmuir* **1998**, *14*, 7140. (o) Dinega, D. P.; Bawendi, M. G. *Angew. Chem., Int. Ed.* **1999**, *38*, 1788. (p) Samia, A. C. S.; Hyzer, K.; Schlueter, J. A.; Qin, C.-J.; Jiang, S.; Bader, S. D.; Lin, X.-M. *J. Am. Chem. Soc.* **2005**, *127*, 4126. (q) Diehl, M. R.; Yu, J.-Y.; Heath, J. R.; Held, G. A.; Doyle, H.; Sun, S.; Murray, C. B. *J. Phys. Chem. B* **2001**, *105*, 7913. (r) Wu, N.; Fu, L.; Su, M.; Aslam, M.; Wong, K. C.; Dravid, V. P. *Nano Lett.* **2004**, *4*, 383.

cobalt organometallic compound under a hydrogen atmosphere in the presence of a mixture of a long-chain amine and an acid.[2b−d] On the other hand, Alivisatos and co-workers synthesized cobalt nanodisks from the thermal decomposition of dicobalt octacarbonyl in hot coordinating surfactants.[2e]

CoO nanocrystals have attracted much attention because they exhibit superparamagnetism or weak ferromagnetism, whereas bulk CoO is antiferromagnetic.[4] Yin and Wang reported the synthesis of tetrahedron-shaped CoO nanocrystals with a size of 4.4 nm by the decomposition of $Co_2(CO)_8$ in toluene under an oxygen atmosphere in the presence of sodium bis(2-ethylhexyl)sulfosuccinate (Na(AOT)).[4b] Chaudret and co-workers synthesized ~2-nm nanoparticles of CoO and Co_3O_4 by the solid-state oxidation of 1.6-nm metallic cobalt nanoparticles.[4c] Rao and co-workers synthesized CoO nanoparticles with sizes ranging from 4 to 18 nm by the decomposition of Co(II) cupferronate in decalin under solvothermal conditions.[4d] Our group[5] and two other groups[6] reported the synthesis of uniformly sized nanocrystals of transition metal oxides by the thermal decomposition of metal−surfactant complexes. In particular, we synthesized short, pencil-shaped CoO nanorods with an unusual wurtzite ZnO structure.[5a] This was the first report on the synthesis of wurtzite ZnO-structured CoO, not only in the form of nanocrystals but also in the bulk form. Later, Park and co-workers also synthesized wurtzite CoO nanocrystals with rod and hexagonal pyramid shapes by the decomposition of Co(acac)$_3$ in oleylamine.[4e] We further extended the synthesis, and herein we report on the synthesis of CoO nanorods with various diameters and lengths and their self-assemblies. Moreover, through their subsequent reduction by heat treatment under a hydrogen atmosphere, orthorhombic Co_2C and hcp Co nanorods were produced. We thoroughly characterized the crystal structures and magnetic properties of the nanorods of CoO, Co_2C, and Co using X-ray absorption (XAS) spectroscopy, X-ray magnetic circular dichroism (XMCD) spectroscopy, and SQUID measurements. We also performed theoretical studies using LDA + U band calculations.

Experimental Section

Synthesis of Co−Oleate Complex. A 9.52 g portion of cobalt chloride hexahydrate ($CoCl_2 \cdot 6H_2O$, 40 mmol, Aldrich Chemical Co., 98%) and 24.36 g of sodium oleate (80 mmol, TCI Co., 95%) were added to a mixture composed of 30 mL of ethanol, 40 mL of distilled water, and 70 mL of *n*-hexane. The resulting mixture solution was heated to 70 °C and maintained at this temperature for 4 h. The solution was then transferred to a separatory funnel, and the upper organic layer containing the Co−oleate complex was washed several times using distilled water. Evaporation of the hexane solvent produced a purple Co−oleate powder.

Synthesis of CoO Nanorods. A 3.12 g portion of the Co−oleate complex (5 mmol) was dissolved in 50 g of 1-octadecene (Aldrich Chemical Co., 90%). The mixture solution was degassed at 120 °C for 2 h under a vacuum to remove the water and oxygen. The solution was then heated to 320 °C with vigorous stirring. The heating rate was controlled to produce CoO nanorods with various aspect ratios. When the reaction temperature reached 320 °C, the initially purple solution became dark green. This color change indicated that the Co−oleate complex was thermally decomposed to generate CoO nanocrystals, whereupon nucleation occurred. The reaction mixture was maintained at this temperature for 30 min to induce sufficient growth. The solution was then cooled to room temperature, and a mixture of acetone and a small fraction of *n*-hexane was added to the solution to yield a waxy precipitate, which was separated by centrifugation. The resulting waxy precipitate was found to be re-dispersible in many organic solvents, such as *n*-hexane and chloroform.

Heat Treatment of CoO Nanorods. For the heat treatment of the CoO nanorods, a Si wafer passivated with a thermally grown SiO_2 layer was used as the substrate to generate a mono- or multilayer thin film. A few drops of a hexane solution containing the CoO nanorods were dropped on the Si wafer. Hexane was then evaporated to generate the self-assembled CoO nanorods. The resulting CoO nanorods, assembled on the Si wafer, were heat-treated at 300 °C for 2 h under a H_2 flow, where the heating rate was 1.56 °C min^{-1} and the H_2 flow rate was 60 mL min^{-1}.

For the large-scale reduction of CoO nanorods, ~2 g of CoO nanorods was loaded in an alumina boat and heat-treated using the same procedure described above.

Characterization of Materials. The nanorods were characterized by low- and high-resolution transmission electron microscopy (TEM), electron diffraction (ED), X-ray diffraction (XRD), X-ray absorption spectroscopy (XAS), and X-ray magnetic circular dichroism (MCD) spectroscopy. The TEM images and electron diffraction patterns were collected on a JEOL JEM-2010 electron microscope. The XRD patterns were obtained using a Rigaku D/Max-3C diffractometer equipped with a rotation anode and a Cu Kα radiation source ($\lambda = 0.15418$ nm). XAS and MCD measurements at the Co $L_{2,3}$-edges were carried out at the EPU6 beamline at the Pohang Light Source. The magnetic properties

(3) (a) Xia, Y.; Yang, P.; Sun, Y.; Wu, Y.; Mayers, B.; Gates, B.; Yin, Y.; Kim, F.; Yan, H. *Adv. Mater.* **2003**, *15*, 353. (b) Cui, Y.; Lieber, C. M. *Science* **2001**, *291*, 851. (c) Huynh, W. U.; Dittmer, J. J.; Alivisatos, A. P. *Science* **2002**, *295*, 2425. (d) Huang, M.; Mao, S.; Feick, H.; Yan, H.; Wu, Y.; Kind, H.; Weber, E.; Russo, R.; Yang, P. *Science* **2001**, *292*, 1897. (e) Cui, Y.; Wei, Q.; Park, H.; Lieber, C. M. *Science* **2001**, *293*, 1289. (f) Gudiksen, M. S.; Lieber, C. M. *J. Am. Chem. Soc.* **2000**, *122*, 8801. (g) Gudiksen, M. S.; Wang, J.; Lieber, C. M. *J. Phys. Chem. B* **2001**, *105*, 4062. (h) Barrelet, C. J.; Wu, Y.; Bell, D. C.; Lieber, C. M. *J. Am. Chem. Soc.* **2003**, *125*, 11498. (i) Hanrath, T. T.; Korgel, B. A. *J. Am. Chem. Soc.* **2002**, *124*, 1424. (j) Holmes, J. D.; Johnston, K. P.; Doty, R. C.; Korgel, B. A. *Science* **2000**, *287*, 1471. (k) Sigman, M. B., Jr.; Ghezelbash, A.; Hanrath, T.; Saunders, A. E.; Lee, F.; Korgel, B. A. *J. Am. Chem. Soc.* **2003**, *125*, 16050. (l) Larsen, T. H.; Sigman, M.; Ghezelbash, A.; Doty, R. C.; Korgel, B. A. *J. Am. Chem. Soc.* **2003**, *125*, 5638. (m) Tang, Z.; Kotov, N. A.; Giersig, M. *Science* **2002**, *297*, 237. (n) Nath, M.; Choudhury, A.; Kundu, A.; Rao, C. N. R. *Adv. Mater.* **2003**, *15*, 2098. (o) Manna, L.; Milliron, D. J.; Meisel, A.; Scher, E. C.; Alivisatos, A. P. *Nat. Mater.* **2003**, *2*, 382. (p) Lee, S.-M.; Cho, S.-N.; Cheon, J. *Adv. Mater.* **2003**, *15*, 441. (q) Hu, J.; Bando, Y.; Liu, Z.; Ahan, J.; Golberg, D.; Sekiguchi, T. *Angew. Chem., Int. Ed.* **2004**, *43*, 63. (r) Park, J.; Koo, B.; Hwang, Y.; Bae, C.; An, K.; Park, J.-G.; Park, H. M.; Hyeon, T. *Angew. Chem., Int. Ed.* **2004**, *43*, 2282. (s) Park, J.; Koo, B.; Yoon, K. Y.; Hwang, Y.; Kang, M.; Park, J.-G.; Hyeon, T. *J. Am. Chem. Soc.* **2005**, *127*, 8433. (t) Song, J. H.; Wu, Y.; Messer, B.; Kind, H.; Yang, P. *J. Am. Chem. Soc.* **2001**, *123*, 10397. (u) Zhang, D.; Liu, Z.; Han, S.; Li, C.; Lei, B.; Stewart, M. P.; Tour, J. M.; Zhou, C. *Nano Lett.* **2004**, *4*, 2151. (v) Woo, K.; Lee, H. J.; Ahn, J.-P.; Park, Y. S. *Adv. Mater.* **2003**, *15*, 1761. (w) Wang, J.; Chen, Q.; Zeng, C.; Hou, B. *Adv. Mater.* **2004**, *16*, 137. (x) Urban, J. J.; Yun, W. S.; Gu, Q.; Park, H. *J. Am. Chem. Soc.* **2002**, *124*, 1186. (y) Gu, G.; Zheng, B.; Han, W. Q.; Roth, S.; Liu, J. *Nano Lett.* **2002**, *2*, 849.

(4) (a) Kodama, R. H. *J. Magn. Magn. Mater.* **1999**, *200*, 359. (b) Yin, J. S.; Wang, Z. L. *J. Phys. Chem.* B **1997**, *101*, 8979. (c) Verelst, M.; Ely, T. O.; Amiens, C.; Snoeck, E.; Lecante, P.; Mosset, A.; Respaud, M.; Broto J. M.; Chaudret, B. *Chem. Mater.* **1999**, *11*, 2702. (d) Ghosh, M.; Sampathkumaran, E. V.; Rao, C. N. R. *Chem. Mater.* **2005**, *17*, 2348. (e) Seo, W. S.; Shim, J. H.; Oh, S. J.; Lee, E. K.; Hur, N. H.; Park J. T. *J. Am. Chem. Soc.* **2005**, *127*, 6188. (f) Xu, C.; Liu, Y.; Xu, G.; Wang, G. *Chem. Phys. Lett.* **2002**, *366*, 567. (g) Zhang, L.; Xue, D.; Gao, C. *J. Magn. Magn. Mater.* **2003**, *267*, 111. (h) Wang, L.; Vu, K.; Navrotsky, A.; Stevens, R.; Woodfield, B. F.; Boerio-Goates, J. *Chem. Mater.* **2004**, *16*, 5394. (i) Flipse, C. F. J.; Rouwelaar, C. B.; de Groot, F. M. F. *Eur. Phys. J. D* **1999**, *9*, 479. (j) Yin, J. S.; Wang, Z. L. *Phys. Rev. Lett.* **1997**, *79*, 2570. (k) Soriano, L.; Abbate, M.; Fernandez, A.; Gonzalez-Elipe, A. R.; Sirotti, F.; Sanz, J. M. *J. Phys. Chem. B* **1999**, *103*,6676. (l) Skumryev, V.; Stoyanov, S.; Zhang, Y.; Hadjipanayis, G.; Givord, D.; Nogues, J. *Nature* **2003**, *423*, 850.

(5) (a) Park, J.; An, K.; Hwang, Y.; Park, J.-G.; Noh, H.-J.; Kim, J.-Y.; Park, J.-H.; Hwang, N.-M.; Hyeon, T. *Nat. Mater.* **2004**, *3*, 891. (b) Choi, S.-H.; Kim, E.-K.; Park, J.; An, K.; Lee, N.; Kim, S.; Hyeon, T. *J. Phys. Chem. B* **2005**, *109*, 14792.

(6) (a) Yu, W. W.; Falkner, J. C.; Yavuz, C. T.; Colvin, V. L. *Chem. Commun.* **2004**, 2306. (b) Jana, N. R.; Chen, Y.; Peng, X. *Chem. Mater.* **2004**, *16*, 3931.

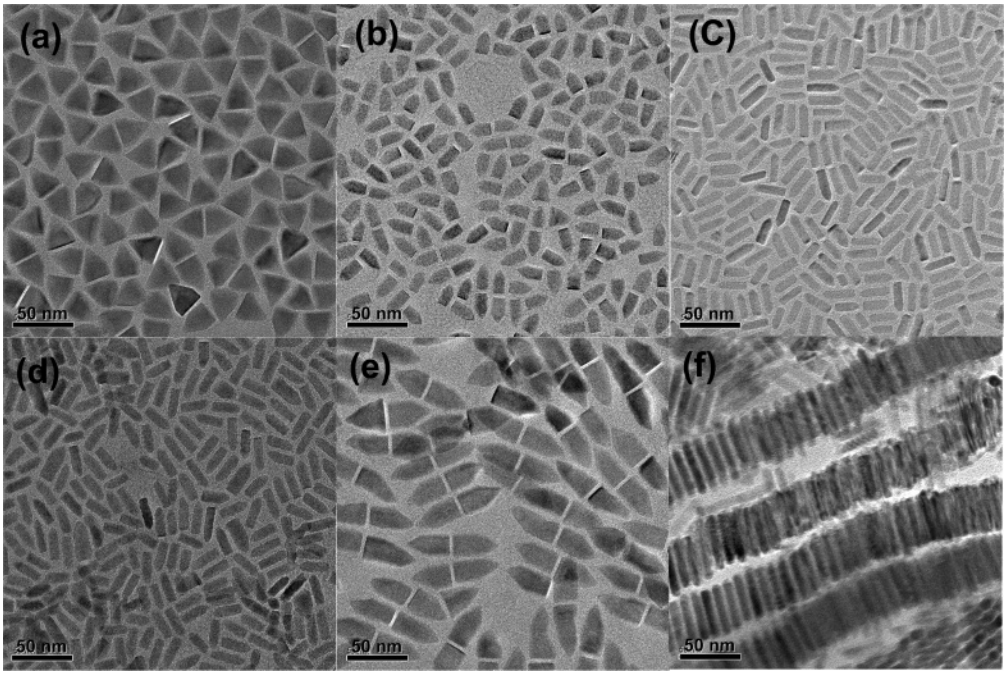

Figure 1. TEM images of pencil-shaped CoO nanorods obtained using various synthetic conditions. CoO nanorods with dimensions of 23 nm (base edge) × 28 nm (height) (a), 12 nm × 19 nm (b), and 8 nm × 26 nm (c), synthesized at heating rates of 3.1, 1.9, and 1.0 °C min^{-1}, respectively, with the same Co−oleate concentration of 5 mmol. CoO nanorods with dimensions of 9 nm × 28 nm (d) and 20 nm × 38 nm (e) were synthesized using 10 and 15 mmol of Co−oleate with the same heating rate of 1.9 °C min^{-1}. (f) 9 nm × 46 nm CoO nanorods were synthesized using the Co−oleate concentration of 5 mmol and a heating rate of 1.9 °C min^{-1}, but an increased aging time of 1 h.

were studied using a magnetic property measurement system (MPMS), 5XL Quantum design SQUID magnetometer, in the temperature range of 5−300 K.

Results and Discussion

Synthesis of CoO Nanorods. CoO nanorods with various aspect ratios were synthesized by the thermal decomposition of a Co−oleate complex in a long-chain hydrocarbon solvent, followed by aging at the reflux temperature. The resulting CoO nanorods were pencil-shaped, with a hexagonal basal plane. The diameters and lengths of the CoO nanorods could be controlled by varying the synthetic parameters, such as the monomer concentration, heating rate, and aging time. The dimensions of the synthesized nanorods are quite uniform, and the size distribution histograms of the nanorods are supplied in the Supporting Information. Figure 1 shows the TEM images of the short, pencil-shaped CoO nanorods with aspect ratios (length/diameter) of 1.22 (Figure 1a), 1.58 (Figure 1b), and 3.25 (Figure 1c), obtained by using different heating rates. When a reaction mixture composed of 5 mmol of Co−oleate complex and 50 g of 1-octadecene was heated to 320 °C at a rate of 3.1 °C min^{-1}, and was subsequently refluxed at this temperature for 30 min, 23 nm (base edge) × 28 nm (height) CoO nanorods were produced (Figure 1a). When the heating rate was decreased to 1.9 and 1.0 °C min^{-1}, 12 nm × 19 nm (Figure 1b) and 8 nm × 26 nm (Figure 1c) CoO nanorods were synthesized, respectively.

As mentioned above, as the heating rate decreased, the aspect ratio of the CoO nanorods increased, whereas the volume of the individual CoO nanorods decreased. The growth rates of the different crystal planes are known to be affected by the heating rates employed during the synthesis of nanocrystals.[7] When sufficient thermal energy is supplied during the synthesis of wurtzite-structured nanocrystals, i.e., a thermodynamically controlled regime, the growth rate along the *c*-axis is generally much higher than that along the other directions, thereby leading to the production of anisotropic rod-shaped nanocrystals.[8] In the current synthesis, when the reaction temperature was slowly increased, long CoO nanorods with a high aspect ratio were produced (Figure 1c). In contrast, short, pencil-shaped CoO nanorods were produced when a high heating rate of 3.1 °C min^{-1} was used (Figure 1a, kinetically controlled regime).

The heating rate also affected the overall size of the nanocrystals. In the current synthesis of nanocrystals, the thermal decomposition of the Co−oleate complex at a certain critical temperature would be expected to generate nuclei.[9] Under fast heating conditions, a relatively small number of nuclei seemed to be generated because of the short nucleation period, consequently producing a small population of large nanocrystals.[10] On the other hand, a large number of small nanocrystals were produced at a low heating rate. As shown in Figure 1, the overall size of the CoO nanorods decreased as the heating rate decreased. The overall size of the nanorods was also increased by increasing the amount of Co−oleate complex while keeping the other experimental conditions unchanged. For example, when the amount of the Co−oleate complex was increased to 10 and 15 mmol at a heating rate of 1.9 °C min^{-1}, 9 nm × 28 nm (Figure 1d) and 20 nm × 38 nm (Figure 1e) CoO nanorods

(7) Song, Q.; Zhang, Z. J. *J. Am. Chem. Soc.* **2004**, *126*, 6164.

(8) (a) Peng, X.; Manna, L.; Yang, W.; Wickham, J.; Scher, E.; Kadavanich, A.; Alivisatos, A. P. *Nature* **2000**, *404*, 59. (b) Chen, Y.; Kim, M.; Lian, G.; Johnson, M. B.; Peng, X. *J. Am. Chem. Soc.* **2005**, *127*, 13331.

(9) (a) Peng, Z. A.; Peng, X. *J. Am. Chem. Soc.* **2002**, *124*, 3343. (b) Yu, W. W.; Peng, X. *Angew. Chem., Int. Ed.* **2002**, *41*, 2368. (c) Park, J.; Privman, V.; Matijevic, E. *J. Phys. Chem. B* **2001**, *105*, 11630. (d) Peng, Z. A.; Peng, X. *J. Am. Chem. Soc.* **2001**, *123*, 1389. (e) Murray, C. B.; Kagan, C. R.; Bawendi, M. G. *Annu. Rev. Mater. Sci.* **2000**, *30*, 545. (f) Jun, Y.-W.; Jung, Y.-Y.; Cheon, J. *J. Am. Chem. Soc.* **2002**, *124*, 615.

(10) Shevchenko, E. V.; Talapin, D. V.; Schnablegger, H.; Kornowski, A.; Festin, O.; Svedlidh, P.; Haase, M.; Weller, H. *J. Am. Chem. Soc.* **2003**, *125*, 9090.

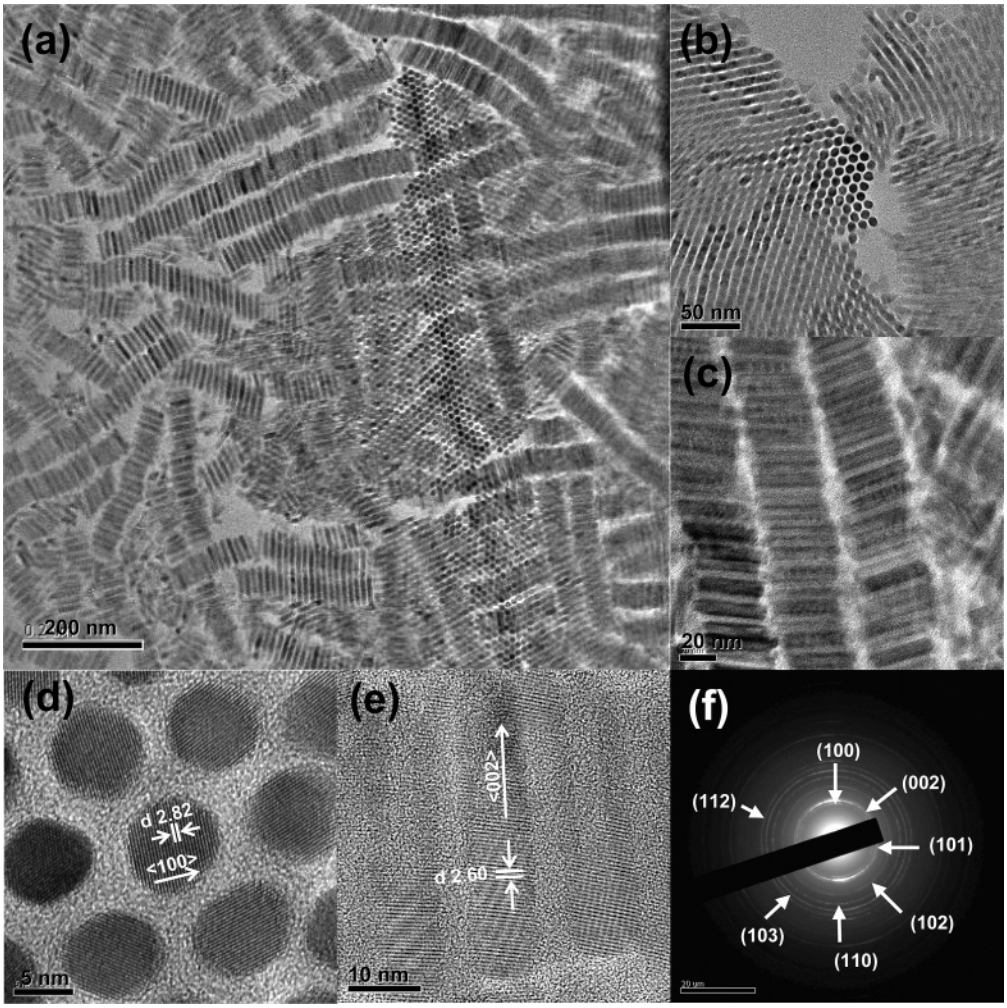

Figure 2. (a) TEM image of the self-assembled CoO nanorods with dimensions of 9 nm × 46 nm. (b,c) TEM images and (d,e) the corresponding high-resolution TEM (HRTEM) images of the top and side views of the parallel-aligned CoO nanorods. (f) Electron diffraction pattern of CoO nanorods.

were produced, respectively. The increased amount of Co−oleate complex seemed to contribute predominantly to the growth source rather than to the nuclei, resulting in the synthesis of increased sized nanorods, which was consistent with the previous synthesis of TiO_2 and CdS nanorods.[11] The size of the CoO nanorods was further controlled by varying the aging time.[12] When the aging time was increased from 30 min to 1 h, the length of the nanorods was increased from 19 nm (Figure 1b) to 46 nm (Figure 1f), while their diameter was decreased slightly.

Self-Assembly. Self-assembly of magnetic nanocrystals, to generate two- and three-dimensional (2-D and 3-D) superlattice structures, is very important both from the viewpoint of the fundamental interest in the collective interaction of nanocrystals and for their potential applications in multi-terabit per square inch magnetic storage media. In particular, the long-range self-assembly of rod-shaped magnetic nanocrystals is of great interest because perpendicular magnetic storage media with increased areal density could potentially be achieved using aligned magnetic nanorod arrays. It is well-known that the size uniformity of nanocrystals is critical to achieve large-area superlattice formation.[13] Self-assembly of the uniform 9 nm × 46 nm CoO nanorods was performed by slowly evaporating a few drops of the hexane solution containing the nanorods on a carbon-coated copper TEM grid. The large area TEM image, shown in Figure 2a, demonstrates that the nanorods self-assembled to form both horizontal parallel arrangements and perpendicular hexagonal honeycomb superlattice structures. The inter-rod distance was 3−4 nm, which corresponds roughly to two layers of the oleic acid surfactant. Figure 2b and c shows the TEM images of the perpendicularly assembled and horizontally assembled arrays, respectively. The high-resolution TEM (HRTEM) image of the perpendicularly aligned nanorods

(11) (a) Cozzoil, P. D.; Kornowski, A.; Weller, H. *J. Am. Chem. Soc.* **2003**, *125*, 14539. (b) Jun, Y.-W.; Lee, S.-M.; Kang, N. J.; Cheon, J. *J. Am. Chem. Soc.* **2001**, *123*, 5150.

(12) Yin, M.; O'Brien, S. *J. Am. Chem. Soc.* **2003**, *125*, 10180.

(13) (a) Murray, C. B.; Kagan, C. R.; Bawendi, M. G. *Science* **1995**, *270*, 1335. (b) Blaarderen A, V.; Ruel, R.; Wiltzius, P. *Nature* **1997**, *385*, 321. (c) Park, J.; Kang, E.; Son, S. U.; Park, H. M.; Lee, M. K.; Kim, J.; Kim, K. W.; Noh, H.-J.; Park, J.-H.; Bae, C. J.; Park, J.-G.; Hyeon, T. *Adv. Mater.* **2005**, *17*, 429. (d) Politi, P.; Pini, M. G. *Phys. Rev. B* **2002**, *66*, 214414. (e) Redl, F. X.; Black, C. T.; Papaefthymiou, G. C.; Sandstrom, R. L.; Yin, M.; Zeng, H.; Murray, C. B.; O'Brien, S. P. *J. Am. Chem.* Soc. **2004**, *126*, 14583. (f) Stoeva, S.; Klabunde, K. J.; Sorensen, C. M.; Dragieva, I. *J. Am. Chem. Soc.* **2002**, *124*, 2305. (g) Stoeva, S.; Prasad, B. L. V.; Uma, S.; Stoimenov, P. K.; Zaikovski, V.; Sorensen, C. M. *J. Phys. Chem. B* **2003**, *107*, 7441. (h) Chen, M.; Nikles, D. E. *Nano Lett.* **2002**, *2*, 211. (i) Wang, Z. L. *Adv. Mater.* **1998**, *10*, 18. (j) Rogach, A. L.; Talapin, D. V.; Shevchenko, E. V.; Kornowski, A.; Haase, M.; Weller, H. *Adv. Funct. Mater.* **2002**, *12*, 653. (k) Shevchenko, E.; Talapin, D.; Kornowski, A.; Wiekhorst, F.; Kötzler, J.; Haase, M.; Rogach, A. L.; Weller, H. *Adv. Mater.* **2002**, *14*, 287. (l) Weller, H. *Philos. Trans. R. Soc. London A* **2003**, *361*, 229. (m) Shevchenko, E. V.; Talapin, D. V.; Rogach, A. L.; Kornowski, A.; Haase, M.; Weller, H. *J. Am. Chem. Soc.* **2002**, *124*, 11480.

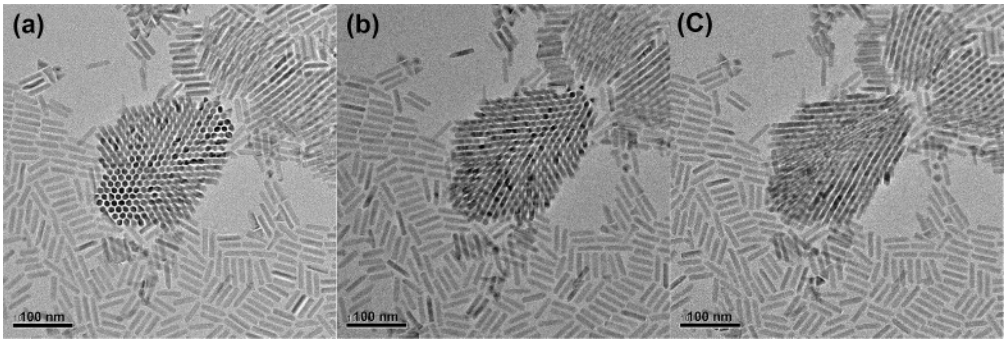

Figure 3. TEM images of CoO nanorods by tilting along the *y*-axis of TEM to confirm the self-assembled nanorod structures. Tilted TEM images obtained at (a) −19°, (b) 0°, and (C) 19° along the *y*-axis, while fixed along the *x*-axis.

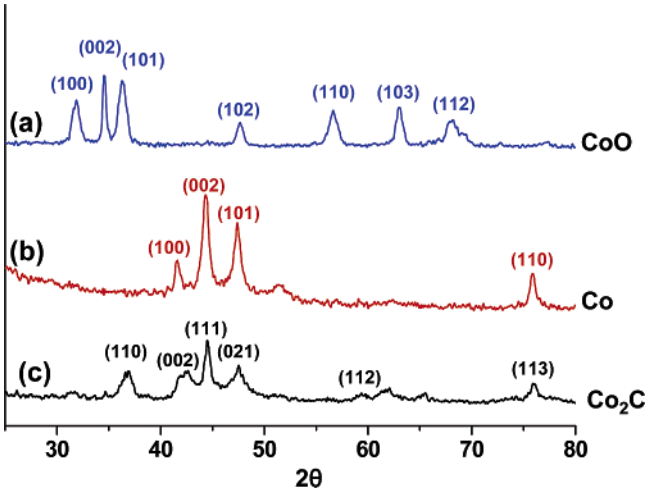

Figure 4. X-ray diffraction (XRD) patterns of (a) CoO nanorods, (b) Co nanorods, and (c) Co_2C nanorods.

showed that the basal plane of the nanorods was the (100) plane, with a calculated *d*-spacing of 2.82 Å. On the other hand, the HRTEM image of the horizontally aligned nanorods showed that the CoO nanorods grew along the [002] direction, with a calculated (002) *d*-spacing of 2.60 Å. These *d*-spacing values matched very well with the standard data. To confirm that the 2-D hexagonal arrays are perpendicularly assembled nanorod arrays rather than assemblies of spherical nanocrystals, a series of tilting experiments were performed. The TEM images, after tilting along the *y*-axis with tilting angles of −19° (Figure 3a), 0° (Figure 3b), and 19° (Figure 3c), clearly demonstrated that the CoO nanorods self-assembled to generate 2-D hexagonal arrays.

Characterization Using XRD. The X-ray diffraction (XRD) pattern of the CoO nanorods, shown in Figure 4a, revealed that the peak positions were identical to the standard wurtzite ZnO pattern ($P6_3mc$, $a = 3.249$ Å, $c = 5.206$ Å, JCPDS No. 36-1451), and the overall pattern was nearly identical to that of the ZnO nanorods reported by our group and other groups.[14] The strikingly intense (002) peak demonstrated the preferential growth of the CoO nanorods along the *c*-axis, which was consistent with the HRTEM data. Although there are many reports on pencil-shaped ZnO crystals with a wurtzite crystal structure, pencil-shaped CoO nanocrystals were only recently reported, first by our research group[5a] and later by Park and co-workers.[4e] Recently, Seshadri and co-workers prepared wurtzite-structured CoO powder.[15] The wurtzite crystal structure is characterized by the hexagonal close-packing of oxygen and metal atoms in space group $P6_3mc$, with metal atoms in the tetrahedral sites.[16] The typical rod-shaped ZnO nanocrystals have a polar basal oxygen plane $(00\bar{1})$ on the bottom of the rods, a top tetrahedron corner-exposed polar metal (001) face, and a low-index face composed of a nonpolar $(\bar{1}00)$ face corresponding to the lateral plane of the rod. The $(00\bar{1})$ plane, which is a low-symmetry nonpolar face with three-fold coordinated atoms, is the most stable, while the polar (001) plane is relatively unstable due to the metal edge. In addition, there is no center of inversion in the wurtzite structure. Consequently, the anisotropic crystal growth along the *c*-axis, leading to the production of pencil-shaped nanorods of ZnO and CoO, seems to be derived from the intrinsic wurtzite crystal structure.[16]

Reduction of CoO Nanorods. We performed the reduction of the self-assembled CoO nanorod arrays to form ferromagnetic nanorod arrays, to investigate their potential application to perpendicular magnetic storage media. When the CoO nanorod arrays, assembled on a silicon substrate, were reduced by heating them at 300 °C for 2 h under flowing H_2, hcp Co nanorods were generated. The XRD pattern (Figure 4b) of the heat-treated sample matched very well with the hexagonal Co structure ($P6_3mmc$, JCPDS No. 05-0727). However, when an alumina boat was used as a container for the large-scale reduction of CoO nanorods, Co_2C nanorods were generated.[17] The XRD pattern in Figure 4c reveals that the final product exhibits an orthorhombic Co_2C structure (*Pmnn*, JCPDS No. 72-1369).[4b] The carbon in the Co_2C nanorods seemed to have been produced from the thermal decomposition of the organic surfactants, which also caused the partially collapsed superlattice structure (Sup-

(14) (a) Joo, J.; Kwon, S. G.; Yu, J. H.; Hyeon, T. *Adv. Mater.* **2005**, *17*, 1873. (b) Miguel, M.; Kahn, M. L.; Maisonnat, A.; Chaudret, B. *Angew. Chem., Int. Ed.* **2003**, *42*, 5321. (c) Yin, M.; Gu, Y.; Kuskovsky, I. L.; Andelman, T.; Zhu, Y.; Neumark, G. F.; O'Brien, S. *J. Am. Chem. Soc.* **2004**, *126*, 6206. (d) Cozzoli, P. D.; Curri, M. L.; Agostiano, A.; Leo, G.; Lomascolo, M. *J. Phys. Chem. B* **2003**, *107*, 4756. (e) Shim, M.; Guyot-Sionnest, P. *J. Am. Chem. Soc.* **2001**, *123*, 11651. (f) Johnson, J. C.; Knutsen, K. P.; Yan, H.; Law, M.; Zhang, Y.; Yang, P.; Saykally, R. J. *Nano Lett.* **2004**, *4*, 197. (g) Greene, L. E.; Law, M.; Tan, D. H.; Montano, M.; Goldberger, J.; Somorjai, G.; Yang, P. *Nano Lett.* **2005**, *5*, 1231. (h) Nyffenegger, R, M.; Craft, B.; Shaaban, M.; Gorer, S.; Erley, G.; Penner, R. M. *Chem. Mater.* **1998**, *10*, 1120.

(15) Risbud, A, S.; Snedeker, L. P.; Elcombe, M. M.; Cheetham, A. K.; Seshadri, R. *Chem. Mater.* **2005**, *17*, 834.

(16) (a) Li, W. J.; Shi, E. W.; Zhong, W. Z.; Yin, Z. W. *J. Cryst. Growth* **1999**, *203*, 186. (b)Vayssieres, L.; Keis, K.; Hagfeldt, A.; Lindquist, S.-E. *Chem. Mater.* **2001**, *13*, 4395. (c) Hu, J. Q.; Li, Q.; Wong, N. B.; Lee, C. S.; Lee, S. T. *Chem. Mater.* **2002**, *14*, 1216. (d) Parker, T. M.; Condon, N. G.; Lindsay, R.; Leibsle, F. M.; Thornton, G. *Surf. Sci.* **1998**, *415*, 1046.

(17) (a)Barriga-Arceo, L. D.; Orozco, E.; Garibay-Febles, V.; Bucio-Galindo, L.; Leon, H. M.; Castillo-Ocampo, P.; Montoya, A. *J. Phys.: Condens. Matter* **2004**, *16*, S2273. (b) Wang, H.; Wong, S. P.; Cheung, W. Y.; Ke, N.; Lau, W. F.; Chiah, M. F.; Zhang, X. X. *Mater. Sci. Eng. C* **2001**, *16*, 147. (c) Liu, B. X.; Wang, J.; Fang Z. Z. *J. Appl. Phys.* **1991**, *69*, 7342.

porting Information). The intense (002) peak of the Co nanorods (Figure 4b) and the (111) peak of the Co_2C nanorods (Figure 4c) demonstrated that the preferential growth characteristics of the CoO nanorods along the *c*-axis of wurtzite structure were retained even after the reduction process.

The facile reduction and the subsequent effective removal of the surfactant from the CoO nanorods assembled on a silicon substrate with a nearly monolayer thickness seemed to be responsible for the production of hcp Co nanorods. On the other hand, the formation of Co_2C nanorods from the large-scale reduction of CoO nanorods can be explained by a retarded removal of a carbon source generated from the decomposition of surfactant. The formation of Co_2C nanoparticles has been well characterized by Wang and co-workers.[4b]

Characterization Using XAS and XMCD. In 1961, Neel suggested that antiferromagnetic materials may become superparamagnetic or weakly ferromagnetic when the particles' size is reduced to the nanometer range, because of the uncompensated number of spins on the two different sublattices.[4a,18] Fcc-structured CoO is one of the representative antiferromagnetic materials.[4] In spite of these interesting magnetic properties, however, it is difficult to obtain pure CoO, because it often contains a small fraction of impurities such as Co_3O_4 or Co metal.[4d] To identify these impurities in the current CoO nanorods, XAS and XMCD measurements at the Co $L_{2,3}$-edges were carried out at the EPU6 beamline at the Pohang Light Source for the 9 nm × 46 nm CoO nanorods (Figure 5). As shown in Figure 5a, the XAS spectrum of the CoO nanorods was very similar to that of bulk CoO. On the other hand, we were able to characterize some of the ferromagnetic impurities by Co $L_{2,3}$-edge XMCD. The XMCD spectra ($\rho+$ and $\rho-$) for the different spin directions, which are parallel and antiparallel to the photon helicity vector, are normalized by the photon flux, and the degree of circular polarization is taken into account in the dichroism signal ($\Delta\rho = \rho+ - \rho-$).[19] In Figure 5b, the MCD line shape was nearly identical to that of Co metal, indicating that the CoO nanorods contain ferromagnetic Co metal impurities. Although the Co $L_{2,3}$-edge XAS spectrum of the nanorods is dominated by that of CoO, the 50-times-enlarged dichroism signal clearly demonstrates the presence of ferromagnetic Co metal impurities.[20] XMCD measurements at the Co $L_{2,3}$-edges were also conducted for the hcp Co and Co_2C nanorods, which were obtained from the reduction of the CoO nanorods (Supporting Information). The MCD spectra of both the hcp Co and Co_2C nanorods showed a line shape very similar to that of typical ferromagnetic metallic Co, although the MCD intensity of the hcp Co nanorods was higher than that of the Co_2C nanorods.

To characterize the magnetic properties of the wurtzite-structured CoO, we carried out first-principles electronic structure calculations[21] based on density functional theory[22] by using the LDA + U method, which is known to be effective in describing transition metal oxides and related systems.[23] The results of the total energy calculations showed that wurtzite CoO

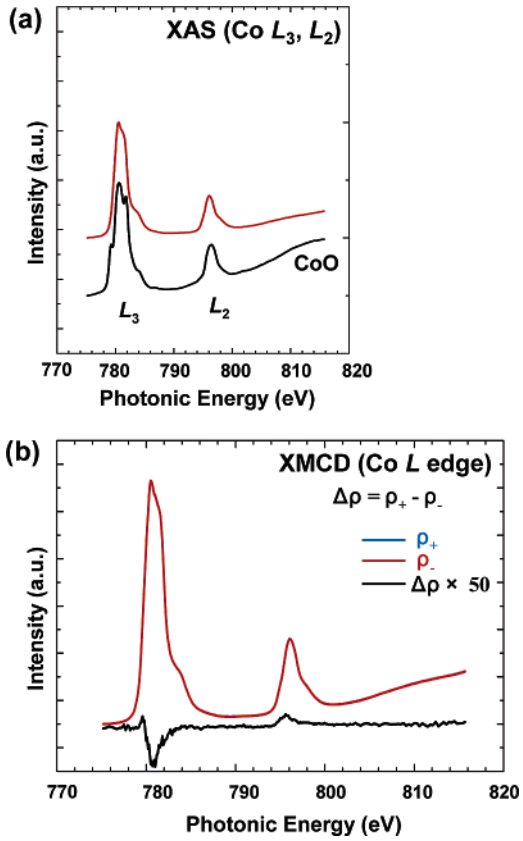

Figure 5. (a) Co $L_{2,3}$-edge XAS spectra of 9 nm × 46 nm CoO nanorods in comparison with bulk CoO. (b) Co $L_{2,3}$-edge XMCD spectrum (upper) and MCD signal (bottom: $\Delta\rho = \rho+ - \rho-$) of 9 nm × 46 nm CoO nanorods. Because XMCD spectra for the two polarization directions are more or less the same in this scale, they appear to overlap in the figure.

favors an A-type antiferromagnetic ground state with layer-by-layer ordered magnetic moments along the *c*-axis direction, similar to the case of bulk fcc CoO. The total energy difference between the ferromagnetic and antiferromagnetic configurations is about 50 meV, regardless of the effective on-site Coulomb parameters that are used. We note that this energy difference of 50 meV between the ferromagnetic and antiferromagnetic configurations of wurtzite CoO is of the same order of magnitude as the value of 117 meV found for bulk fcc CoO, which provides further evidence that wurtzite CoO has an antiferromagnetic ground state. Consequently, the XMCD results, combined with the band structure calculations, suggested that the small ferromagnetic magnetic signal observed in the XMCD spectra represents not the intrinsic characteristics of wurtzite CoO but rather the existence of a small fraction of Co metal impurities in the CoO nanorods.

Magnetic Characterization. We measured the temperature and field dependences of the magnetization curves using a commercial superconducting quantum interference device (SQUID) magnetometer. Zero-field-cooling (ZFC) and field-

(18) Neel, L. *C. R. Hebd. Seances Acad. Sci.* **1961**, *252*, 4075.
(19) (a) Chen, C. T.; Idzerda, Y. U.; Lin, H.-J.; Smith, N. V.; Meigs, G.; Chanban, E.; Ho, C. H.; Pellergin, E.; Sette, F. *Phys. Rev. Lett.* **1995**, *75*, 152. (b) Groot, F. M. F.; Fuggle, J. C.; Thole, B. T.; Sawatzky, G. A. *Phys. Rev. B* **1990**, *42*, 5459.
(20) Kim, J.-Y.; Park, J.-H.; Park, B.-G.; Noh, H.-J.; Oh, S.-J.; Yang, J. S.; Kim, D.-H.; Bu, S. D.; Noh, T.-W.; Lin, H.-J.; Hsieh, H.-H.; Chen, C. T. *Phys. Rev. Lett.* **2003**, *90*, 017401-1.
(21) We have performed the calculation for the periodic unit cell of wurtzite CoO by using our open MX LDA + U code (http://staff.aist.go.jp/t-ozaki/openmx), developed for the nanomaterials study. We employed a Troullier−Martins-type pseudopotential with partial-core corrections and adopted 216 *k*-points for the Brillouin zone integration. All the calculational parameters used in this study have been extensively tested and checked for the bulk fcc CoO as a reference.
(22) (a) Hohenberg, P.; Kohn, W. *Phys. Rev.* **1964**, *136*, 864. (b) Kohn, W.; Sham, L. J. *Phys. Rev.* **1965**, *140*, 1133.
(23) Anisimov, V. I. *Strong Coulomb correlations in electronic structure calculation*; Gordon and Breach Science Publishers: Amsterdam, 2000.

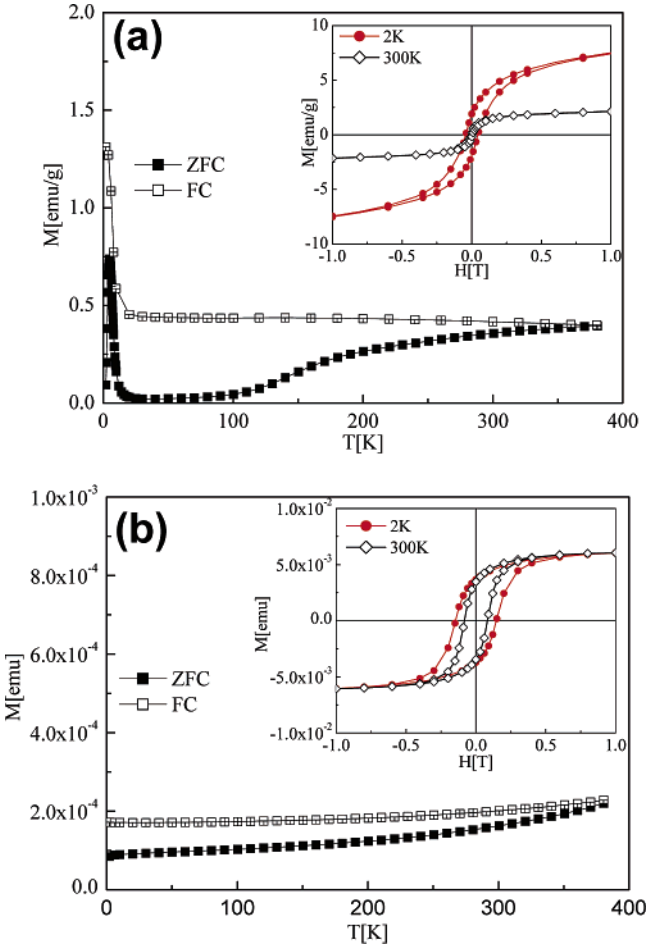

Figure 6. (a) Temperature dependence of magnetization for 9 nm × 46 nm CoO nanorods measured with applied field of 100 Oe after zero-field-cooling (filled circles) and field-cooling (open circles). The inset shows the field dependence of the magnetization taken at 2 and 300 K. (b) Temperature dependence of magnetization for 9 nm × 46 nm Co nanorods after heat treatment, measured with an applied field of 100 Oe after zero-field-cooling (filled circles) and field-cooling (open circles). The inset exhibits the field dependence of the magnetization of CoO nanorods at 2 and 300 K. Since we prepared samples on top of Si substrate for heat treatment, we show here only the raw data without converting them into the magnetization per unit mass.

cooling (FC) measurements are known to be a useful way of determining the so-called blocking temperature of magnetic nanomaterials. In principle, nanomaterials of pure antiferromagnetic compounds cannot show a blocking behavior unless there are abnormal surface states. In a few antiferromagnetic nanomaterials, such surface states are indeed known to exhibit a blocking phenomenon in ZFC/FC measurements similar to those of superparamagnetic nanoparticles. Figure 6a shows the typical data for the 9 nm × 46 nm CoO nanorods before the heat treatment, measured with an applied field of 100 Oe after ZFC (filled circles) and FC (open circles). As shown in Figure 6a, the FC data deviate from the ZFC data well above 300 K, although the ZFC data decrease rather smoothly before the temperature reaches 200 K. Upon further cooling, the ZFC data show a peak centered at 5 K, and the FC data start to increase in approximately the same temperature range. We observed similar features, including the low-temperature peak in the ZFC data, in other samples measured under the same conditions before the heat treatment. We speculate that the origin of the low-temperature peak has nothing to do with the wurtzite CoO phase. Interestingly enough, it was recently reported that 20-nm Co_3O_4 nanoparticles exhibit a sharp peak structure in the ZFC data near 25 K.[24] Thus, it may not be too unrealistic to suppose that smaller Co_3O_4 nanoparticles have the same peak structure at lower temperatures as that observed in our sample. It is also worthwhile to note that similar peak structures were observed in the magnetization data of MnO nanoparticles, which was found to be due to Mn_3O_4 impurity phases.[25] We found that, in the field dependence of the magnetization, shown in the inset of Figure 6a, there is a clear, albeit small, hysteresis in the data taken at 2 K, which weakens upon warming. There are two more things we need to discuss about the data presented in Figure 6a. The first comment concerns the irreversible point in the FC and ZFC data. If we take it as a blocking temperature of the wurtzite CoO, it basically implies that CoO nanorods should have abnormal surface states since simple antiferromagnetic nanoparticles cannot give rise to such a blocking behavior. Although our LDA + U band calculations predict that wurtzite CoO has an antiferromagnetic ground state with an energy difference of 50 meV between antiferromagnetic (AF) and ferromagnetic states, it is not very unusual that nanoparticles with supposedly AF states show blocking behavior due to uncompensated surface magnetic states. That the saturated magnetic moment in the inset is 7 emu/g, somewhat smaller than that of fcc CoO, may be due to either weaker magnetic properties of wurtzite CoO compared with fcc CoO or, more probably, an error in our estimate of sample mass without including surfactant mass correctly. The second comment is about the temperature dependence, in particular that below 100 K. Although the observed behavior is not entirely explainable by wurtzite CoO with uncompensated surface spin states, it is also true that the temperature dependence of our magnetization data may be contaminated by some small magnetic impurity. Therefore, we caution ourselves against interpreting the data solely on the basis of intrinsic properties of wurtize CoO, although we believe that the major part of the data should come from wurtize CoO simply because it is far larger in volume compared with other impurities. Closely related to this, Seshadri et al. synthesized wurtzite CoO crystals by a nonaqueous solution route.[15] They showed that their wurtzite CoO contained Co metal impurity and its magnetic properties were affected by the ferromagnetic Co impurity.

We also measured the magnetization curves after the reduction process. As shown in Figure 6b, there is a deviation between the FC and ZFC data at a slightly higher temperature compared with the data taken before the heat treatment. Another noticeable effect is that the low-temperature peak structure is absent in the heat-treated sample. Similarly, the magnetic hysteresis is observed to be much stronger, as shown in the inset of Figure 6b, compared with the data obtained before the heat treatment. This rather drastic effect of the heat treatment can be understood in terms of Co clustering. As described above, the ferromagnetic signal observed in our XMCD results is most likely due to the Co metal clusters present in the CoO nanorods, in which case the most obvious heat treatment effect would be the clustering of Co. In fact, a similar Co clustering effect has been found in Co-implanted anatase TiO_2 thin films with increasing annealing temperature.[26] Therefore, we believe that the rather high

(24) Makhlouf, S. A. *J. Magn. Magn. Mater.* **2002**, *246*, 184.
(25) Park, J.; Kang, E.; Bae, C. J.; Park, J.-G.; Noh, H.-J.; Kim, J.-Y.; Park, J.-H.; Park, H. M.; Hyeon, T. *J. Phys. Chem. B* **2004**, *108*, 13594.

blocking temperature observed both before and after the heat treatment, as well as the marked changes found in the magnetic properties after heat treatment, arises from Co clusters and may not be entirely due to the wurtzite CoO phase, which is in agreement with the XMCD results and the band structure calculations.

Conclusions

In summary, we synthesized uniformly sized, pencil-shaped CoO nanorods with a wurtzite crystal structure by the thermal decomposition of a cobalt−oleate complex. The dimensions of the CoO nanorods were easily controlled by changing the synthetic parameters, such as the heating rate, the amount of Co−oleate complex, and the aging time. Due to their size uniformity, the nanorods self-assembled to form both horizontal parallel arrangements and perpendicular hexagonal honeycomb superlattice structures. Reduction of the CoO nanorods produced either hcp Co nanorods or Co_2C nanorods. The well-aligned arrays of the resulting Co_2C and Co nanorods could potentially be used as high-areal-density perpendicular magnetic storage media. The current synthetic procedure is very simple and highly reproducible and, consequently, is readily applicable to large-scale synthesis for potential industrial applications. For example, when 12.5 g of the Co−oleate complex (20 mmol) was used in the synthesis, 4.6 g of uniformly sized CoO nanorods was produced (Supporting Information).

Acknowledgment. T.H. thanks the Korean Ministry of Science and Technology for financial support through the National Creative Research Initiative Program of the Korea Science and Engineering Foundation (KOSEF). J.G.P. and J.Y. thank the KOSEF for financial support through the Center for Strongly Correlated Materials Research at the Seoul National University. J.H.P. thanks KISTEP for financial support through the X-ray/particle-beam Nanocharacterization Program.

Supporting Information Available: Photograph showing a balance weighing CoO nanorods and particle size distribution histograms; TEM and HRTEM images of Co_2C nanorods; XMCD and MCD spectra of Co and Co_2C nanorods. This material is available free of charge via the Internet at http://pubs.acs.org.

JA0608702

(26) Kim, D. H.; Yang, J. S.; Kim, K. S.; Kim, D.-W.; Noh, T. W.; Bu, S. D.; Kim, Y.-W.; Park, Y. D.; Pearton, S. J.; Jo, J.; Park, J.-G. *Appl. Phys. Lett.* **2003**, *83*, 4574.